

Notes to

Climate Changes

By

MLK

Advisor: Prof. [TBD]

Committee: Profs. [TBD]

Department of Mathematics

My Place

September 14, 2023

TABLE OF CONTENTS

1	The governing system of equations	1
1.1	The primitive equations	1
1.2	Separating unresolved turbulence effects	3
1.3	Approximations to the equations	6
1.3.1	Hydrostatic Approximation	6
1.3.2	Boussinesq and anelastic approximation	6
1.3.3	Shallow fluid equation	7
1.4	Initial and boundary conditions	10
2	Solar variability and climate change	11
2.1	Main causes of solar variability	11
3	Statistical assessments of anthropogenic factor on Climate change	16
3.1	Data and Results	16
4	Changes in the TSI and climatic effect	18
4.1	Foreword	18
5	Climate Change and Its Causes	24
5.1	Climate change – another perspective	24

6	Recent changes in solar outputs and GMST	30
6.1	Analysis of contributions to GMAST	30
7	Empirical analysis of the solar contribution to GMAST change	34
7.1	An empirical climate model with short and long characteristic time responses .	34
	References	39
	Appendices	40
A	Main constants used in climate analysis	40
B	Main greenhouse gas constants	41
C	Main formulae used in climate analysis	43
D	Radiative Forcing induced by main greenhouse gases¹	44
E	Note about climate sensitivity parameter	45

CHAPTER 1

THE GOVERNING SYSTEM OF EQUATIONS

1.1 The primitive equations

The basic equations are as follows and will be described below

$$\frac{\partial u}{\partial t} = -u \frac{\partial u}{\partial x} - v \frac{\partial u}{\partial y} - w \frac{\partial u}{\partial z} + \frac{u \tan \varphi}{a} - \frac{u w}{a} - \frac{1}{\rho} \frac{\partial p}{\partial x} - 2\Omega(w \cos \varphi - v \sin \varphi) + Fr_x \quad (1.1)$$

$$\frac{\partial v}{\partial t} = -u \frac{\partial v}{\partial x} - v \frac{\partial v}{\partial y} - w \frac{\partial v}{\partial z} - \frac{u^2 \tan \varphi}{a} - \frac{u v}{a} - \frac{1}{\rho} \frac{\partial p}{\partial y} - 2\Omega u \sin \varphi + Fr_y \quad (1.2)$$

$$\frac{\partial w}{\partial t} = -u \frac{\partial w}{\partial x} - v \frac{\partial w}{\partial y} - w \frac{\partial w}{\partial z} - \frac{u^2 + v^2}{a} - \frac{1}{\rho} \frac{\partial p}{\partial z} - 2\Omega u \cos \varphi - g + Fr_z \quad (1.3)$$

$$\frac{\partial T}{\partial t} = -u \frac{\partial T}{\partial x} - v \frac{\partial T}{\partial y} + (\gamma - \gamma_d)w + \frac{1}{c_p} \frac{dH}{dt} \quad (1.4)$$

$$\frac{\partial \rho}{\partial t} = -u \frac{\partial \rho}{\partial x} - v \frac{\partial \rho}{\partial y} - w \frac{\partial \rho}{\partial z} - \rho \left(\frac{\partial u}{\partial x} + \frac{\partial v}{\partial y} + \frac{\partial w}{\partial z} \right) \quad (1.5)$$

$$\frac{\partial q_v}{\partial t} = -u \frac{\partial q_v}{\partial x} - v \frac{\partial q_v}{\partial y} - w \frac{\partial q_v}{\partial z} + Q_v \quad (1.6)$$

$$P = \rho R T \quad (1.7)$$

Description of the equations:

- equations (1.1-3) represent the momentum equations of a spherical Earth, that is, Newton's second law of motion which states that the rate of change of momentum of a body is proportional to the resultant force acting on the body, and in the same direction of the force;
- equation (1.4) is the thermodynamic energy equation accounting for various effects, both adiabatic and diabatic, on temperature;
- equation (1.5) is the continuity equation for total mass, that states that the mass is neither gained nor destroyed, while equation (1.6) is the same, but applied to water vapor only;
- equation (1.7) is the ideal gas law, which relates pressure, temperature and density.

The variables used have the following meaning:

- u, v, w are the Cartesian velocity components;
- p is the pressure;
- ρ is the density;
- T is the temperature;
- q_v is the specific humidity;
- Ω is the rotational frequency of Earth (angular velocity);
- φ is the latitude;
- a is the Earth's radius;
- γ is the lapse rate of temperature; ¹
- γ_d is the dry adiabatic lapse rate; ²
- c_p is the specific heat of air at constant temperature;
- g is the acceleration of gravity;
- H represents a gain or loss in heat;
- Q_v is the gain or loss of water vapour through phase changes;
- Fr is a generic friction term in each coordinate direction.

¹The lapse rate of temperature refers to the rate at which temperature changes with altitude in the Earth's atmosphere. It is the rate of decrease in temperature with increasing altitude. Standard lapse rate, aka environmental lapse rate, is approximately 6.5 °C per kilometre for the lower atmosphere. This means that, on average, for every kilometre of altitude gained, the temperature decreases by about 6.5 °C. Actual lapse rate can vary depending on factors such as humidity, air pressure, and the time of day.

²The dry adiabatic lapse rate refers to the rate at which a parcel of dry (unsaturated) air cools as it rises in the atmosphere, without exchanging heat with its surroundings. This rate of cooling is purely due to the expansion of the air as it rises and experiences a decrease in pressure. The dry adiabatic lapse rate is approximately 9.8 °C per kilometre. This means that, on average, a parcel of dry air will cool by about 9.8 °C for every kilometre of altitude gained, as long as it remains unsaturated.

1.2 Separating unresolved turbulence effects

The above equations apply to all scales of motions, even waves and turbulence that are too small to be represented by models designed for weather processes. These equations must be revised as the turbulence cannot be revealed explicitly in such models. To do that, it is possible to split all the dependent variables into mean and turbulence parts, that is, spatially resolved and unresolved components.

The mean is defined as the average over a grid cell [15], e.g.

$$\begin{aligned} u &= \bar{u} + u', \\ T &= \bar{T} + T', \\ p &= \bar{p} + p'. \end{aligned}$$

These expression can be substituted into the primitive equations above. Let us take equation (1.1), we have,

$$u \frac{\partial u}{\partial x} = (\bar{u} + u') \frac{\partial}{\partial x} (\bar{u} + u') = \bar{u} \frac{\partial \bar{u}}{\partial x} + \bar{u} \frac{\partial u'}{\partial x} + u' \frac{\partial \bar{u}}{\partial x} + u' \frac{\partial u'}{\partial x} \quad (1.8)$$

referring to the mean motion implies to apply the average to all terms, that is,

$$\overline{u \frac{\partial u}{\partial x}} = \overline{\bar{u} \frac{\partial \bar{u}}{\partial x}} + \overline{\bar{u} \frac{\partial u'}{\partial x}} + \overline{u' \frac{\partial \bar{u}}{\partial x}} + \overline{u' \frac{\partial u'}{\partial x}}, \quad (1.9)$$

the last term on the right is a term of covariance, that is, when positive values for u' tend to be paired with negative values of $\frac{\partial u'}{\partial x}$, the covariance and the relative term would be negative, in case the two parts are not physically correlated, the mean has a value of zero. In this context the equation can be simplified using Reynold's postulate [16], therefore,

$$\overline{u \frac{\partial u}{\partial x}} = \overline{\bar{u} \frac{\partial \bar{u}}{\partial x}} + \overline{u' \frac{\partial u'}{\partial x}}, \quad (1.10)$$

keeping in mind that, for what we said,

$$\begin{aligned}\overline{u'} &= 0 \implies \overline{u} \frac{\partial \overline{u'}}{\partial x} = 0 \implies \\ \overline{\frac{\partial u'}{\partial x}} &= \overline{\overline{u}} \frac{\partial \overline{u'}}{\partial x} = \overline{u} \frac{\partial \overline{u'}}{\partial x} = 0, \\ \overline{u' \frac{\partial u'}{\partial x}} &= 0.\end{aligned}$$

The equation (1.1) can be typically represented including a frictional term Fr_x , without Earth's curvature term and only with a determinant Coriolis term,

$$\frac{\partial u}{\partial t} = -u \frac{\partial u}{\partial x} - v \frac{\partial u}{\partial y} - w \frac{\partial u}{\partial z} - \frac{1}{\rho} \frac{\partial p}{\partial x} + f_v + \frac{1}{\rho} \left(\frac{\partial \tau_{xx}}{\partial x} + \frac{\partial \tau_{yx}}{\partial y} + \frac{\partial \tau_{zx}}{\partial z} \right), \quad (1.11)$$

where τ_{zx} is the force per unit area, or momentum, or shearing stress, exerted in the x direction by the fluid of one side of a constant- z plane with its opposite side, same for τ_{xx} and τ_{yx} for the relative coordinate planes.

In case of inviscid fluids, there would be no action between the flow on either side of the planes. Fluids in reality show a molecular motion or molecular diffusion which affects the coordinate surfaces. In these equations, which explicitly represent turbulence motion, subgrid friction is due to viscous forces only, as a consequence of molecular motion; a typical representation for the stress is

$$\tau_{zx} = \mu \frac{\partial u}{\partial x},$$

where μ is the coefficient of viscosity. Substituting this expression into the equation (1.11) for the Newtonian friction,

$$\frac{\partial u}{\partial t} \propto \frac{1}{\rho} \left(\mu \frac{\partial^2 u}{\partial x^2} + \mu \frac{\partial^2 u}{\partial y^2} + \mu \frac{\partial^2 u}{\partial z^2} \right) = \frac{\mu}{\rho} \nabla^2 u.$$

Applying the averaging process, with $\rho' \ll \rho$,

$$\frac{\partial \overline{u}}{\partial t} = -\overline{u} \frac{\partial \overline{u}}{\partial x} - \overline{v} \frac{\partial \overline{u}}{\partial y} - \overline{w} \frac{\partial \overline{u}}{\partial z} - \frac{1}{\rho} \frac{\partial \overline{p}}{\partial x} + \overline{f_v} - \overline{u' \frac{\partial u'}{\partial x}} - \overline{v' \frac{\partial u'}{\partial y}} - \overline{w' \frac{\partial u'}{\partial z}} + \frac{1}{\rho} \left(\frac{\partial \overline{\tau}_{xx}}{\partial x} + \frac{\partial \overline{\tau}_{yx}}{\partial y} + \frac{\partial \overline{\tau}_{zx}}{\partial z} \right). \quad (1.12)$$

For turbulence scale motion, the following continuity equation holds,

$$\frac{\partial u'}{\partial x} + \frac{\partial v'}{\partial y} + \frac{\partial w'}{\partial z} = 0.$$

taking the average, multiplying by u' and adding to equation (1.12), we get,

$$\frac{\partial \bar{u}}{\partial t} = -\bar{u} \frac{\partial \bar{u}}{\partial x} - \bar{v} \frac{\partial \bar{u}}{\partial y} - \bar{w} \frac{\partial \bar{u}}{\partial z} - \frac{1}{\rho} \frac{\partial \bar{p}}{\partial x} + \bar{f}_v - \frac{\overline{\partial u' u'}}{\partial x} - \frac{\overline{\partial u' v'}}{\partial y} - \frac{\overline{\partial u' w'}}{\partial z} + \frac{1}{\rho} \left(\frac{\partial \bar{\tau}_{xx}}{\partial x} + \frac{\partial \bar{\tau}_{yx}}{\partial y} + \frac{\partial \bar{\tau}_{zx}}{\partial z} \right). \quad (1.13)$$

By analogy with the molecular-viscosity related stresses, we can define the turbulent stresses as follows,

$$T_{xx} = -\overline{\rho u' u'},$$

$$T_{yx} = -\overline{\rho u' v'},$$

$$T_{xz} = -\overline{\rho u' w'},$$

we obtain,

$$\frac{\partial \bar{u}}{\partial t} = -\bar{u} \frac{\partial \bar{u}}{\partial x} - \bar{v} \frac{\partial \bar{u}}{\partial y} - \bar{w} \frac{\partial \bar{u}}{\partial z} - \frac{1}{\rho} \frac{\partial \bar{p}}{\partial x} + \bar{f}_v - \frac{1}{\rho} \left[\frac{\partial}{\partial x} (\tau_{xx} + T_{xx}) + \frac{\partial}{\partial y} (\tau_{yx} + T_{yx}) + \frac{\partial}{\partial z} (\tau_{zx} + T_{zx}) \right], \quad (1.14)$$

which is basically the same as equation (1.11). It is worth noting that the mean-value symbols are rarely used with the primitive equations³, but it is still understood that the dependant variables represent only nonturbulant motions. Moreover, turbulent stresses, often symbolically represented by F , as friction, are much larger than the viscous stresses, so the latter terms are usually not included in the model.

³This terminology is used to distinguish these model from ones that are based on differentiated versions of the equations.

1.3 Approximations to the equations

1.3.1 Hydrostatic Approximation

Sound waves are generally of no meteorological importance, this can help to simplify the model, using equations in a form that does not admit them.

A possible approach is to employ the hydrostatic approximation wherein the complete third equation of motion (1.3) is replaced by one containing only gravity and vertical-pressure-gradient terms, that is,

$$\frac{\partial p}{\partial z} = -\rho g,$$

which implies that the density is tied to the vertical pressure gradient.

Actually, sound waves are not possible in a hydrostatic atmosphere as they require longitudinal compression and expansion within the waves.

In order the hydrostatic assumption to be valid, the sum of all terms eliminated in the complete equation needs to be an order of magnitude smaller than the term retained, thus,

$$\left| \frac{\partial w}{\partial t} \right| \ll g.$$

1.3.2 Boussinesq and anelastic approximation

These approximations, as with the hydrostatic approximation, are part of a family to filter sound waves from the equations by decoupling the pressure and density perturbations.

The Boussinesq approximation is obtained by substituting the following for equation (1.5), the complete continuity equation,

$$\frac{\partial u}{\partial x} + \frac{\partial v}{\partial y} + \frac{\partial w}{\partial z} = 0,$$

this amounts to substituting volume conservation to mass conservation.

For anelastic approximation the equation

$$\frac{\partial}{\partial x}(\bar{\rho}u) + \frac{\partial}{\partial y}(\bar{\rho}v) + \frac{\partial}{\partial z}(\bar{\rho}w) = 0,$$

is substituting for the complete continuity equation, where $\bar{\rho} = \bar{\rho}(z)$ is a steady reference-state density.

1.3.3 Shallow fluid equation

This refers to the fact that the wavelengths simulated need to be long relative to the depth of the fluid. In this case, the fluid should be auto-barotropic⁴, homogeneous⁵, incompressible⁶, hydrostatic and inviscid.

The equations from which we begin derivation are,

$$\frac{\partial u}{\partial t} + u \frac{\partial u}{\partial x} + v \frac{\partial u}{\partial y} + w \frac{\partial u}{\partial z} - f_v + \frac{1}{\rho} \frac{\partial p}{\partial x} = 0 \quad (1.15)$$

$$\frac{\partial v}{\partial t} + u \frac{\partial v}{\partial x} + v \frac{\partial v}{\partial y} + w \frac{\partial v}{\partial z} + f_u + \frac{1}{\rho} \frac{\partial p}{\partial y} = 0 \quad (1.16)$$

$$\frac{\partial \rho}{\partial z} = -\rho g \quad (1.17)$$

$$\frac{\partial \rho}{\partial t} + \rho \left(\frac{\partial u}{\partial x} + \frac{\partial v}{\partial y} + \frac{\partial w}{\partial z} \right) = 0. \quad (1.18)$$

Incompressibility and homogeneity mean $\frac{\partial \rho}{\partial t} = 0 \implies \rho = \rho_0 = \text{constant}$ and

$$\frac{\partial u}{\partial x} + \frac{\partial v}{\partial y} + \frac{\partial w}{\partial z} = 0, \quad (1.19)$$

⁴The state of a fluid in which surfaces of constant density (or temperature) are coincident with surfaces of constant pressure.

⁵Density does not vary in space.

⁶Density does not change in time following a parcel.

in addition,

$$\frac{\partial p}{\partial z} = -\rho_0 g, \quad (1.20)$$

that is,

$$\frac{\partial}{\partial x} \left(\frac{\partial p}{\partial z} \right) = \frac{\partial}{\partial x} (-\rho_0 g) = 0,$$

which means that there is no horizontal variation of the vertical pressure gradient or vertical variation of the horizontal pressure gradient (definition of barotropy).

Now, as pressure-gradient force generates wind, and the resulting Coriolis force, all forces are invariant with the height.

Integrating equation (1.20) over the depth of the fluid (P_S and P_T are the pressures at the bottom and at the top of the fluid respectively), we get,

$$\int_{z(P_S)}^{z(P_T)} \frac{\partial p}{\partial z} dz = -\rho_0 g \int_{z(P_S)}^{z(P_T)} dz \implies \\ P_S - P_T = g\rho_0 h,$$

where h is the height of the fluid.

If $P_T = 0$ or $P_T \ll P_S \implies \frac{P_S}{\rho_0} = g h \implies \frac{1}{\rho_0} \frac{\partial P_S}{\partial x} = g \frac{\partial h}{\partial x}$, the horizontal pressure gradient at the bottom of the fluid is proportional to the gradient in the depth of the fluid, this can allow to give to the equations (1.15) and (1.16) a new form for the pressure-gradient term.

Equation (1.19) can be also integrated with respect to z ,

$$\int_0^z \frac{\partial w}{\partial z} dz = w_z - w_s = - \int_0^z \left(\frac{\partial u}{\partial x} + \frac{\partial v}{\partial y} \right) dz.$$

If u and v are not initially functions of z , we obtain,

$$w_h - w_s = - \left(\frac{\partial u}{\partial x} + \frac{\partial v}{\partial y} \right) h, \quad z = h.$$

For a horizontal lower boundary condition, kinematic condition $w_s = 0$ prevails.

In addition, recognizing that

$$w_h = \frac{dh}{dt}$$

leads to a new continuity equation. We then have in the three variables u , v and h

$$\begin{aligned}\frac{\partial u}{\partial t} + u \frac{\partial u}{\partial x} + v \frac{\partial u}{\partial y} + w \frac{\partial u}{\partial z} - f_v + g \frac{\partial h}{\partial x} &= 0 \\ \frac{\partial v}{\partial t} + u \frac{\partial v}{\partial x} + v \frac{\partial v}{\partial y} + w \frac{\partial v}{\partial z} + f_u + g \frac{\partial h}{\partial y} &= 0 \\ \frac{\partial h}{\partial t} + u \frac{\partial h}{\partial x} + v \frac{\partial h}{\partial y} + \left(\frac{\partial u}{\partial x} + \frac{\partial v}{\partial y} \right) h &= 0.\end{aligned}$$

A ne-dimensional set of equations can be written as follows

$$\begin{aligned}\frac{\partial u}{\partial t} + u \frac{\partial u}{\partial x} - f_v + g \frac{\partial h}{\partial x} &= 0, \\ \frac{\partial v}{\partial t} + u \frac{\partial v}{\partial x} + f_u + g \frac{\partial h}{\partial y} &= 0, \\ \frac{\partial h}{\partial t} + u \frac{\partial h}{\partial x} + v \frac{\partial h}{\partial y} + h \frac{\partial u}{\partial x} &= 0, \\ \frac{\partial H}{\partial t} &= -\frac{f}{g} \bar{U},\end{aligned}$$

where \bar{U} represents the constant mean geostrophic speed on which u perturbation is superimposed.

Of course, this model has limitation to represent the real atmosphere, but one step forward is to define fluid depth to be consistent with the layer being represented, such as the boundary level or the troposphere. The depth of the total atmosphere can be represented by the scale height

$$H = \frac{RT_0}{g},$$

where T_0 is the surface temperature and $H \approx 8$ km.

When the above non-linear shallow-fluid equations are used as the basis for a model, an explicit numerical diffusion term will need to be added to each equation to suppress the short wavelengths

that will grow through the aliasing process, more information in [5] and [11].

1.4 Initial and boundary conditions

[TO BE DEVELOPED]

CHAPTER 2

SOLAR VARIABILITY AND CLIMATE CHANGE¹

2.1 Main causes of solar variability

There are two main sources that can affect the solar radiation in time, on one hand the internal processes, which can impact on the radiant energy emitted and can be described as solar activity; on the other hand, changes on Earth's orbit around the Sun over very long period of tens to hundreds of thousands of years, which can directly affect the amount of energy hitting the Earth and its distribution around the globe.

These changes can affect climate, annual and decadal variations in solar activity are correlated with sunspot activity. Sunspots numbers have been observed and recorded over hundreds of years. Whilst in millennial timescales variations of solar activity can be found in ice cores, tree rings, ocean sediments. With the help of a careful statistical analysis, it is possible to reveal decadal or centennial signals of solar variability in climate data.

For much longer timescales, signs of solar variations can be seen as the trigger for glacial-interglacial transitions, with their effect amplified with feedback mechanisms, such as the following cycle:

TSI² increases \Rightarrow temperature of the planet increases \Rightarrow CH₄ and CO₂ increase in oceans and icecaps \Rightarrow GHGs³ produce additional warming; this is what is called a positive feedback. Currently the idea in fashion, is that it is not probably possible to explain global warming with the only activity of the Sun in the last 60 years. Over the past 150 years an overall solar activity has probably contributed to global warming, but the effect is estimated to be much smaller than the total net of human forcing of the climate system through emissions of GHGs and other factors.

¹Haigh J., Solar influence on Climate (article), 2011, Imperial College London.

²TSI = Total Solar Irradiance

³GHG = Greenhouse Gas

Nevertheless, this is still an area of active research and more investigation is required to have a clearer view of the actual factors involved in these changes.

The solar flux mainly depends on three key parameters relative to Earth, the eccentricity of its orbit (currently 0.0034, varying with periods of around 100,000 and 413,000 years), the precession of the seasons (which varies with a period up to 26,000 years) and the obliquity (tilt) of its axis (currently 23.5° and varying with a period of about 41,000 years). The elliptical orbit of the Earth causes the solar irradiance S , at a latitude φ , to vary during the year, an approximate value can be given by the following equation,

$$S \approx S_0 \left(1 + 0.034 \cdot \cos \frac{2\pi n}{365.25} \right) \cos \varphi,$$

where n is the number of a day in a year and $S_0 = 1366 \text{ Wm}^{-2}$ is the solar constant.

On very long timescales the solar irradiance can be altered by variation in these orbital parameters and the amount of energy arriving in summer at high altitudes determines whether the winter growth of the ice cap will recede or the climate can be turned into a ice age. Together with TSI, the number of sunspots has been carefully recorded in the last four centuries, shown an 11-year cycle during which there is a growing and decaying of SSN. Of particular note is the period near the end of the 17th century (approx. 1675-1715) where the number declined to near zero for several decades (the Maunder Minimum), the low activity near the start of the 19th century (the Dalton Minimum) and the relatively high activity over the most recent fifty years.

Another proxy indicator is the number of aurorae, which are produced by high energetic particles in the solar wind, interacting with the atmosphere and are more frequently observed when the Sun is more active.

The solar wind and the solar magnetic field provide protection for the Earth from galactic cosmic rays (GCRs), which are high energy charged particles originating outside the solar system. There is an inverse relationship between solar activity and the incidence of GCRs. Solar activity can be derived from surface measurements of neutrons produced by the impact of GCRs on the

atmosphere.

The proxy measures discussed above provide useful signals of solar activity but there is no clear indication of the physical processes over possible solar influence on the climate. Of course, TSI is the most obvious candidate as a mechanism that can affect variation on the Earth atmosphere; the measurements provided by different instruments show consistent variations of approximately 0.08% ($\approx 1.1 \text{ Wm}^{-2}$) in TSI over an 11-year cycle, but significant uncertainties remain with regards to the absolute value of TSI with a discordance of about 1 Wm^{-2} .

To assess the potential influence of the Sun on the climate on longer timescales it is necessary to know TSI further back into the past. There are several different approaches taken to *reconstructing* the TSI, all employing a substantial level of empiricism and in all of which the proxy data (such as SSN) are calibrated against the recent satellite TSI measurements. These estimates diverge as they go back in time due to the different assumptions made about the state of the Sun during the Maunder Minimum in the latter part of the 17th century. A useful parameter, in assessing climate change impact of different factors, is Radiative Forcing (RF). This gives a measure of the imbalance in the radiation budget at the top of the atmosphere caused by a particular factor. For instance, the introduction of increasing concentrations of GHGs traps outgoing heat radiation, increasing the net energy flow into the Earth's atmosphere and therefore implying a positive RF. Conversely, an increase in amount of radiation reflected back to space, due to an enhancement in the area of reflective surfaces such as ice caps or white clouds over the sea, would result in a negative RF.

The Intergovernmental Panel on Climate Change (IPCC) summarises RF since 1750 due to *anthropogenic* factors with a positive RF totalling about 2.5 Wm^{-2} . A key concern of contemporary climate science is to attribute causes, including the contribution of solar variability, to the observed variations in temperature. The simplest approach is to calculate the correlation of the time series of temperature with that of the factor of interest. Another commonly used approach is that of multiple linear regression analysis which seeks to derive simultaneously the magnitude of signals due to a number of pre-determined factors.

On millennial timescales changes in the Earth's orbit, as well as, variations in solar activity, must be considered; initial warming is assumed due to an increase in solar irradiance, but the amplification would also take place in response to any other factor initiating a warming, such as GHGs produced by human activity.

On shorter timescales, hundreds of years, changes in the Earth's orbit can be disregarded; directly observed climate records suggesting that the climate has been changing over the past century include the retreat in mountain glaciers, sea level rise, thin Arctic ice sheets and an increased frequency of extreme precipitations events. Sun may have introduced an overall global warming of approximately 0.07 °C before 1960 but had a little effect since. Over the whole period the temperature has increased by about 1 °C, so the fractional contribution ascribed to the Sun is consistent to the proportions shown below.

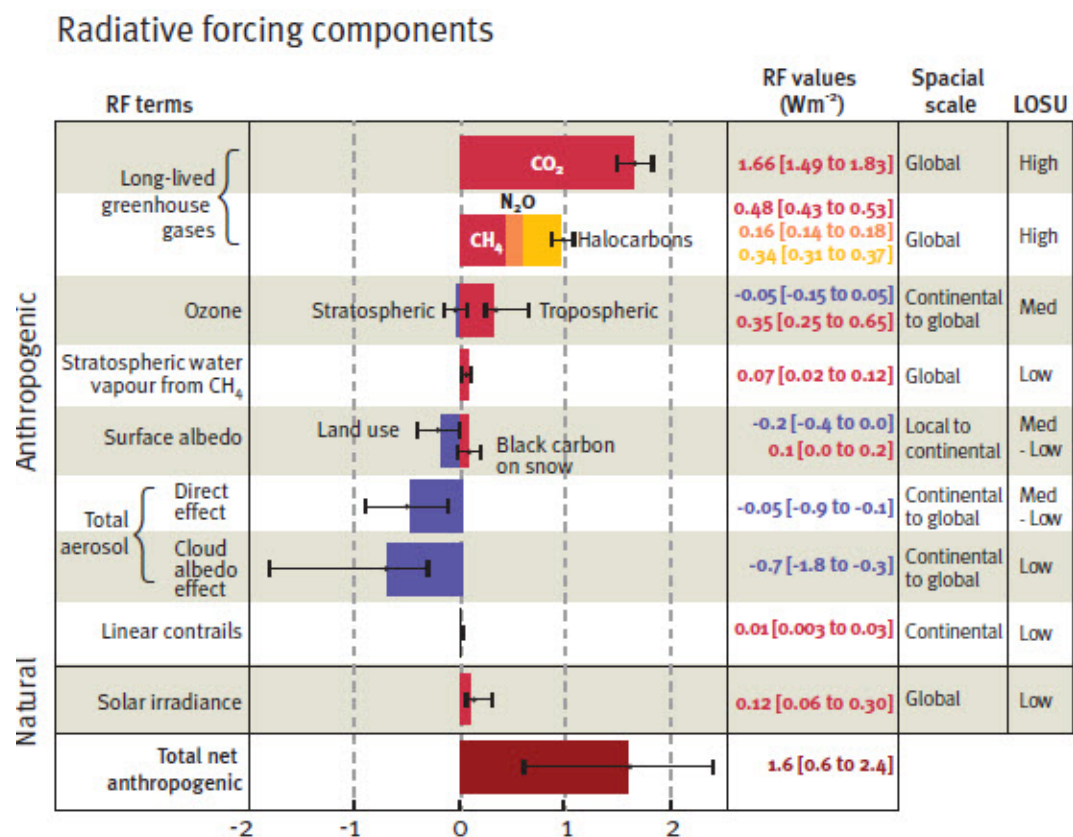


Figure 2.1: Radiative Forcing (Wm⁻²)

It is not possible to reproduce the global warming of recent decades without including anthropogenic effects and this is confirmed by those using more sophisticated non-linear statistical techniques; the separation of effects of natural and anthropogenic forcing suggest that the solar contribution is particularly significant to the observed warming over the period 1900-1940, however, the models cannot reproduce the warming over the past few decades with natural factors alone [19].

One recent multiple regression analysis of factors influencing sea surface temperatures shows very little 11-year solar cycle signal in the tropics but significant impacts in mid-latitudes. With regards to sea surface temperatures the mechanisms are usually thought to be “bottom-up” in the sense that solar radiation heats the sea surface and the atmosphere responds through thermodynamic processes which impact the hydrological cycle, tropical climate and ocean circulations.

Other mechanisms proposed to explain the influence of solar activity on the lower atmosphere, referred to as “top-down”, involve dynamical influences between the upper and lower layers of the atmosphere.

Clouds play a major part in establishing the heat and radiation budget of the atmosphere. They transport latent heat from the ocean to the atmosphere and have a large effect on the Earth’s radiation balance. They reflect about 15% of the incoming solar radiation acting in a similar way to GHGs to warm the surface. Thin high clouds (at altitude greater than about 6 km) generally generate a net heating effect, and thick low clouds (altitude below 2 km) produce a cooling.

Another mechanism involving responses in cloudiness to solar-induced changes in atmospheric ionisation by galactic cosmic rays (GCRs) requires more evidence before any of the proposed pathways can be considered both operational and effective.

CHAPTER 3

STATISTICAL ASSESSMENTS OF ANTHROPOGENIC AND NATURAL GLOBAL CLIMATE FORCING¹

3.1 Data and Results

All statistical analyses refer to the physical background as provided by RF calculations [21].

The annual global mean surface air temperature data (TGL) are provided by CRU (2009)² called HadCRUT3. Natural forcing is represented by solar activity (SOL), explosive volcanism (VOL), and ENSO (El Niño / southern oscillation). In case of SOL, the solar irradiation reconstruction provide by [7] is used. Volcanic forcing, due to explosive eruptions reaching the stratosphere, is described in terms of annual forcing data. These data³ are globally averaged and approximately extrapolated by means of the VEI (volcanic explosive index) data, available from the US Smithsonian Institution (2009)⁴. The mean time lag between volcanic eruptions and temperature effects (related to annual data) amount to one year and is realized in the forcing data. ENSO data, in terms of SOI (southern oscillation index) are again from CRU (2009)⁵.

Anthropogenic forcing is represented by GHGs and SUL (sulphate aerosols). As far as GHGs are concerned, CO₂ equivalents⁶ are used for additional gases.

Note that the scientific understanding of aerosol forcing is still low; although it is known to be a considerable time lag of temperature response, particularly, to GHGs forcing, the temperature effect can be observed every year and it is known it may be due to GHGs forcing some decades before.

¹Schönwiese C. D., Walter A., Brinckmann A. W., Statistical assessments of anthropogenic and natural global climate forcing. An update (article), 2010, Meteorologische Zeitschrift.

²Climate Research Unit, UK.

³www.juergen-grieser.de/downloads/VolcanicAerosolForcing/VolcanicAerosolForcing.htm.

⁴Global Volcanic program, <https://volcano.si.edu/>.

⁵Climatic Research Unit, UK. <https://crudata.uea.ac.uk/cru/data/soi/>.

⁶CO₂-eq = Gt (gross tons of a gas) · GWP (Global Warming Potential value of the gas). E.g. for Methane (CH₄) the GWP value is 25, for Nitrous oxide (NO₂) is 265.

The most simple statistical model to match any effects with any forcing factors is multiple linear regression (MLR). The most important presuppositions of MLR is that the forcing factors should be independent from each other and the unexplained residuum should be Gaussian distributed. Most climate mechanisms are of a non-linear nature, therefore, non-linear regression techniques must be used.

The data analysis can show that the anthropogenic forcing has become a dominant effect in recent time, whereas in earlier time natural and anthropogenic forcing have acted at a similar level of magnitude. The regression analysis is able to reproduce the observed climate variations at high level and to discern between anthropogenic and natural signals.

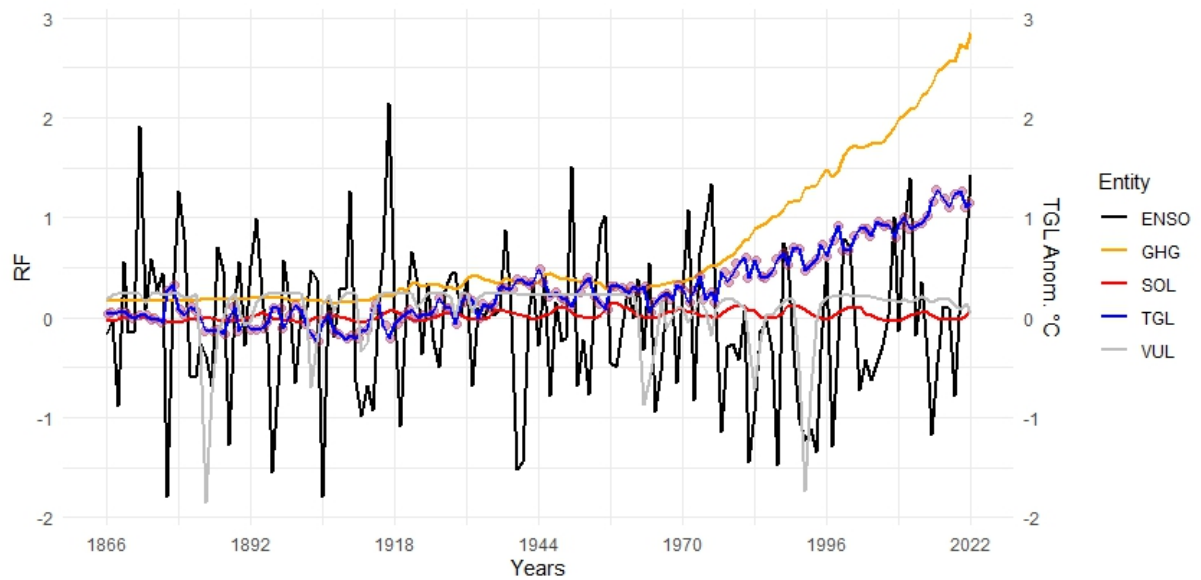


Figure 3.1: RF and temperature (anomaly °C) for TGL

CHAPTER 4

CHANGES IN TOTAL SOLAR IRRADIANCE AND CLIMATIC EFFECT¹

4.1 Foreword

On a global scale, historic 100-year-long climate excursions cannot be scientifically identified with significance. Despite these substantial uncertainties, records attest to a *mild* period in Europe from the years 950-1100 and of *cold winters*, at least in northern Europe, in the 16th to 17th centuries. According to the 100 000-year orbital forcing scenario, the last *abrupt* onset of the warming occurred some 10 000 years ago, making the world enter the so called *Holocene*. Since this maximum, orbital forcing has slowly been decreasing. In temperature records, these effects were highest 6000 to 9000 years before the present time and have decreased since then to a minimum during the most recent pre-industrial time.

Since there is no significant variation in orbital forcing on timescales of 100 or 1000 years, variations in climate may be induced by other phenomena. The influence most commonly proposed by *experts*² are either large volcano eruptions or solar radiative variations or both.

Given that the volcanic frequency deduced from sulfate concentration in ice from Antarctica does not support a volcano-only climate forcing, it appears that there is a need for additional influence. It is still an open question to identify this additional influence, but solar radiance seems to be a good candidate.

A well-known example of a volcanic influence is the eruption of Mount Tambora in Indonesia, on April 10, 1815, which is most probably responsible for the *year without summer* in the year following the eruption. But in addition to this identifiable influence in 1816, there was a cool period reported for the northern hemisphere from about 1800 to 1820 that started earlier than

¹Schmutz W. K., Changes in Total Solar Irradiance and climatic effect. *J Space Weather Space Clim.* **11**, 40. <https://www.doi.org/10.1051/swsc/2021016>

²Anyway, who these real experts can be is not properly clear.

Tambora eruption. Even though another localized eruption was reported to have happened in 1809, the cold period extended longer than the effects of both eruptions should have lasted.

At the same time, there was a period of reduced solar activity, which can be identified using proxies of the solar activity, e.g. reduced sunspot group numbers. This low solar activity period, lasting from 1790 to 1860, is called the Dalton minimum. Modelling efforts advocate that the effect of both forcings are needed – volcanic and reduced solar irradiance – to explain the reported cooler climate during the Dalton minimum.

While there is a widespread agreement that there is a relationship between climatic and solar activity variations on the 100 to 1000-year timescale, opinions start to diverge when it comes to identifying the physical reason and quantifying a potential solar influence. Some scientists argue that observed solar irradiance since 1979 has not varied in its basic level. Thus, they exclude the possibility of reduced solar irradiance values and any direct influence of solar irradiance on climate in the past.

Because TSI is the energy input to Earth, an accurate measurement record of the spectrally integrated TSI arriving at the top of the atmosphere is very important for the assessment of the Earth climate system. A good estimation of TSI from 1979 to present are the measurements of Total Solar Irradiance Spacecraft Total Irradiance Monitor³ (TSIS/TIM).

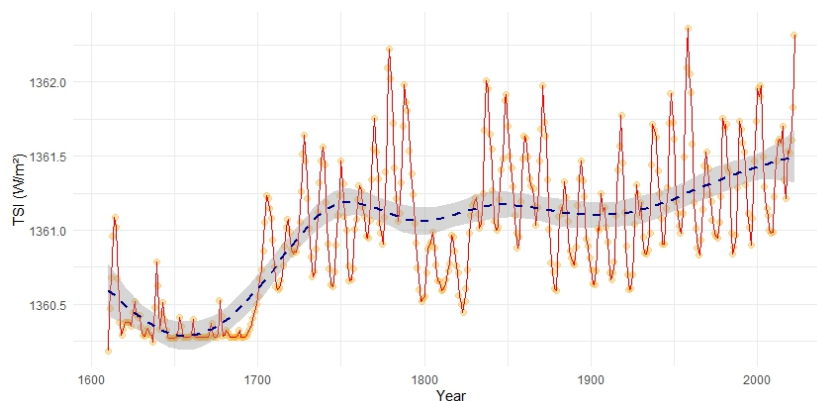


Figure 4.1: TSI trend 1610-2022 with smooth line

³Historical Total Solar Irradiance Reconstruction, 1610-2018: https://lasp.colorado.edu/lisird/data/historical_tsi. And TSIS-1, 2018-present: <https://lasp.colorado.edu/tsis/data/tsi-data/>

The PMOD-composite⁴ [4] suggests that there was a decline of 0.1 Wm^{-2} between TSI-minima in 1985 and 2017 (marked in the chart below), whereas the blue TSI-composite line yields a decline of 0.2 Wm^{-2} between 1985 to 2019. Neither trend is significant as the uncertainties of the records, about $0.1 \text{ Wm}^2/10 \text{ yr}$, have large magnitudes. The result is that currently, it is not possible to be confident of any multi-decadal trend in TSI.

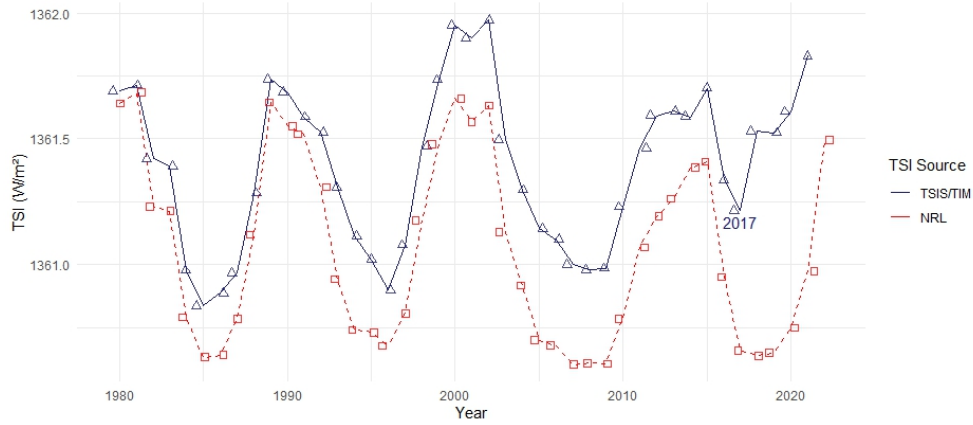


Figure 4.2: TSI time series 1980-2022 according with two different sources

To quantify the direct solar influence we use the textbook formula for the terrestrial energy balance

$$\pi R_{\oplus}^2 S_{\odot} (1 - \mathcal{A}_{\oplus} - \alpha) = 4\pi R_{\oplus}^2 \sigma T_{\oplus}^4 (1 - \mathcal{G}_{\text{eff}}), \quad (4.1)$$

where the LHS is the solar energy that reaches the earth ground level and the RHS gives the outgoing radiation energy. T_{\oplus} is the average earth surface temperature, R_{\oplus} is the Earth's radius and S_{\odot} is the total solar irradiance received on the Earth at the average distance of 1 AU from the Sun. \mathcal{A}_{\oplus} denotes the terrestrial albedo, α the absorption of radiation when passing down through the atmosphere, and \mathcal{G}_{eff} stands for an effective *greenhouse* effect that includes everything of Earth's highly complex climate system. The average solar irradiance over the past three decades is $S_{\odot} = 1361 \text{ Wm}^{-2}$. The albedo and the atmospheric absorption are given as $\mathcal{A}_{\oplus} = 29.4\%$ and

⁴Best estimate composite of TSI from the beginning of space era in 1979 until 2003.

$\alpha = 23.5\%$ in the glbal energy balance diagrams [25]. In order to get the current average Earth's surface temperature, 288 K, the effective *greenhouse* effect is $\mathcal{G}_{\text{eff}} = 59\%$.

The climate sensitivity to a varying solar irradiance is given by

$$\frac{\partial T_{\oplus}}{\partial S_{\odot}} = \frac{\partial}{\partial S_{\odot}} \left[\left(\frac{1 - \mathcal{A}_{\oplus} - \alpha}{4\sigma(1 - \mathcal{G}_{\text{eff}})} \right)^{1/4} \right] \cdot S_{\odot}^{1/4} + \left(\frac{1 - \mathcal{A}_{\oplus} - \alpha}{4\sigma(1 - \mathcal{G}_{\text{eff}})} \right)^{1/4} \cdot \frac{\partial(S^{1/4})}{\partial S_{\odot}}, \quad (4.2)$$

where the first term is indirect solar forcing and the second term is direct solar forcing. Assuming that the parameters \mathcal{A}_{\oplus} , α and \mathcal{G}_{eff} of the equation for the global energy balance are not affected by a variation of the solar irradiance, that is, $\frac{\partial \mathcal{A}_{\oplus}}{\partial S_{\odot}} = \frac{\partial \alpha}{\partial S_{\odot}} = \frac{\partial \mathcal{G}_{\text{eff}}}{\partial S_{\odot}} = 0$, we have, given (4.1) and the above condition for the parameters

$$\begin{aligned} T_{\oplus}^4 &= \frac{1 - \mathcal{A}_{\oplus} - \alpha}{4\sigma(1 - \mathcal{G}_{\text{eff}})} S_{\odot} \implies T_{\oplus} = \left[\frac{1 - \mathcal{A}_{\oplus} - \alpha}{4\sigma(1 - \mathcal{G}_{\text{eff}})} \right]^{1/4} \cdot S_{\odot}^{1/4} = \mu \cdot S_{\odot}^{1/4}, \text{ where } \mu = \left[\frac{1 - \mathcal{A}_{\oplus} - \alpha}{4\sigma(1 - \mathcal{G}_{\text{eff}})} \right]^{1/4} \implies \\ \frac{\partial T_{\oplus}}{\partial S_{\odot}} &= \mu \cdot \frac{\partial(S_{\odot}^{1/4})}{\partial S_{\odot}} = \frac{1}{4} \mu \frac{\partial S_{\odot}}{S_{\odot}^{3/4}} = \frac{1}{4} \mu \frac{\partial S_{\odot}}{S_{\odot}^{3/4}} \cdot \frac{S_{\odot}^{1/4}}{S_{\odot}^{1/4}} = \frac{1}{4} \left(\mu \cdot S_{\odot}^{1/4} \right) \cdot \frac{\partial S_{\odot}}{S_{\odot}} = \frac{1}{4} T_{\oplus} \frac{\partial S_{\odot}}{S_{\odot}} \implies \\ \frac{\partial T_{\oplus}}{T_{\oplus}} &= \frac{1}{4} \frac{\partial S_{\odot}}{S_{\odot}} \implies \partial T_{\oplus} = \frac{T_{\oplus}}{4 S_{\odot}} \partial S_{\odot} \implies \\ \partial T_{\oplus} &= f \partial S_{\odot}, \end{aligned} \quad (4.3)$$

where $f = \frac{288}{4 \times 1361} = 0.053 \text{ K}/(\text{Wm}^{-2})$, the sensitivity parameter to variations of the solar irradiance for the present day values of T_{\oplus} and S_{\odot} as given above.⁵

The largest observed *radiance* variations by the sun result from the passage of very large sunspot groups. In space era, the largest observed decrease in TSI was in October 2003 with a reduction of 0.34%, corresponding to 4.6 Wm^2 . According to equation (4.3), this forces a decrease of 1/4 K (or 1/4 °C) of Earth's mean temperature. This forcing lasts only few day, that is, probably, this is not detectable in global temperature records.

The largest measured *irradiance* variations result from the eccentric orbit of Earth. The current

⁵In climate sciences, the incoming solar energy is usually related to the total Earth's surface and thus, the solar irradiance is divided by a factor of four, $\hat{S}_{\odot} = S_{\odot}/4 = 340 \text{ Wm}^{-2}$, which yields a climate sensitivity $\partial T_{\oplus} = \hat{f} \partial \hat{S}_{\odot}$, with a factor of four larger numeric value $\hat{f} = 0.21 \text{ K}/(\text{Wm}^{-2})$.

value of eccentricity is $e = 0.0167$ [24], which yields a ration of aphelion to perihelion distances of $(1 + e)/(1 - e) = 1.034$ that makes the solar irradiance measured at Earth vary from 1316 Wm^{-2} in July (aphelion) to 1407 Wm^{-2} in January (perihelion), which would make the global temperature vary almost 5°C over the year.

Yearly averages of TSI are well correlated with the yearly average of the sunspot number (SSN) ($R \approx 0.94$), therefore, as in the Maunder minimum in 17th century the SSN is almost zero, it is possible to assume that TSI has almost a constant value at $\text{SSN} = 0$, that is, $\text{TSI}_{\text{SSN}=0} \approx 1360.5 \text{ Wm}^{-2}$ over decades during the Maunder minimum. Compared to the present day 21-year TSI average, $\text{TSI}_{(21\text{-year})} \approx 1361.0 \text{ Wm}^{-2}$, this is 0.5 Wm^{-2} lower, which means that, using the above equation (4.3), leads to a decrease of $\approx 0.04^\circ\text{C}$. Therefore, in order to force $\approx 1^\circ\text{C}$ cooler temperature, during the Maunder minimum, the contribution from the term for indirect solar forcing, the first term at RHS of equation (4.2) had to be 30-times larger than the direct solar forcing term. Thus, indirect forcing by non-zero partial derivatives of the parameters \mathcal{A}_\oplus , α and \mathcal{G}_{eff} , had to dominate the proposed climate change.

The climate literature refers to two ways of amplifying direct TSI-forcing, termed “Bottom-Up” and “Top-Down” mechanisms. As the terms suggest, the first involves a reaction of the sea temperature, which is inherently a slow process that takes years to develop, whereas the second mechanism takes place in higher atmospheric layers with all processes being fast.

A Fourier transformation of annual global near-surface temperature [14], detrended for global warming with a third-degree polynomial, shows a peak with a period of 9.1 years over the 11-year solar cycle period. However, it not clear whether this peak can be related to solar cycle forcing; evidence for a relation to solar cycle forcing is that this periodicity has an amplitude of 0.05°C , which is anticipated from forcing by 1 Wm^{-2} direct forcing.

From the energy conservation equation of the Earth system (4.1), the effect of solar variability on climate has two terms: a direct effect that relates a variation in TSI to the global temperature and a term, which summarizes many potential non-linear influences on Earth’s climate. An important characteristic of amplification is whether it is a fast reaction that should show up immediately or

it needs time to build up. All processes in the atmosphere are fast in the sense that new status is established within minutes for radiative processes and within hours to days for atmospheric waves and wind patterns. In fact, in higher atmospheric layers the Top-down mechanism is easily detected. If it existed, a large amplification of direct forcing by Top-down mechanism on near-surface temperature would be observable, in particular amplifying the huge annual variation due to eccentric Earth orbit about the Sun. From the missing impact of solar irradiance variations with timescales shorter than months, it can be concluded that the Top-down mechanism does not have a significant impact on the global surface temperature.

For the Bottom-up effect, the direct forcing has to build up with time to make an integrated difference in energy compared to the large energy content of the ocean. If the forcing is large enough, e.g. for large volcanic events that yield a global reduction in atmospheric transmission due to their aerosol emissions, there are reported observable effects on climate. Thus, it is possible to understand that within one or two years a TSI forcing is detectable. From at-best marginally detected solar cycle influence on near-surface temperatures, apparently, a large amplification of the direct forcing does not exist; neither for Top-down nor for Bottom-up mechanisms.

CHAPTER 5

CLIMATE CHANGE AND ITS CAUSES¹

5.1 Climate change – another perspective

Since 1900 the global surface temperature of the Earth has risen by about 0.8 °C, and since the 70s by about 0.5 °C, as shown by the below chart.

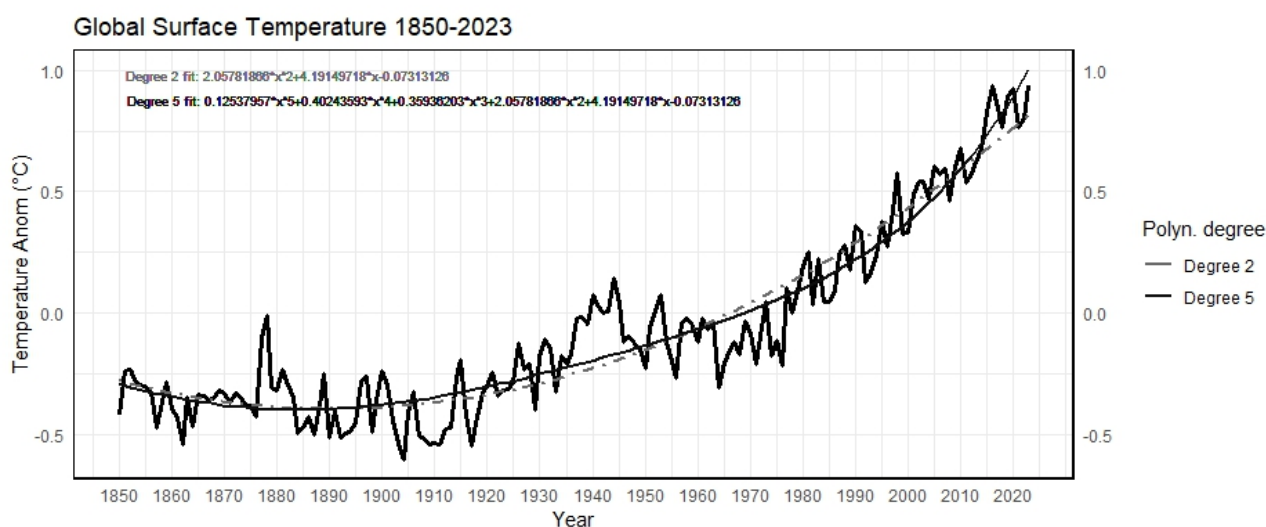


Figure 5.1: GMAST 1850-2023

This temperature increase occurred during a significant atmospheric concentration increase of some GHGs, especially CO₂ and CH₄, which is known to be mainly due to human emissions. According to the *Anthropogenic Global Warming Theory* (AGWT) humans have caused more than 90% of global warming (GW) since 1900 and virtually 100% of GW since 1970. The AGWT is currently advocated by the International Panel on Climate Change (IPCC), however, not everyone shares the IPCC's views. The climate system is more complex than what is now known, several

¹Scafetta N., Climate Change and Its Causes. A Discussion about Some Key Issues *SPPI Original Paper* (2010) <https://www.epa.gov/environmental-economics/climate-change-and-its-causes-discussion-about-some-key-issues>

mechanisms are not yet included in the climate models considered by the IPCC and that this issue should be treated with some caution because incorrect environmental policies could also cause extensive damage.

The existence of an anthropogenic bias appears evident in Figure 2.1 that shows the complete list of radiative forcings, which, as the IPCC claims, have caused GW observed since 1750. This figure divides the climatic forcings into two groups: one group includes only the total solar irradiance and it is labeled *natural*, the other group comprises the rest and it is labeled *anthropogenic*. Thus, the IPCC claims that 100% of the increase the CO₂ and CH₄ atmospheric concentrations observed since 1750 and the change of all other climate components, except for the TSI, are *anthropogenic*. These labels do suggest that without humans the chemical concentrations of the atmosphere and the number of other climatic parameters would remain rigorously unchanged despite a change of the solar energetic input!

This claim is not physical because as the solar activity increases, climate warms, and this causes a net increase of atmospheric CO₂ and CH₄ concentrations. During warming the ability of the ocean to absorb these gases from the atmosphere decreases because of Henry's law² is the partial pressure of the gas (often in units of atm) and other mechanisms. A warming would also increase the natural production of atmospheric CO₂ and CH₄ on the land due to the fermentation of organic material, outgassing of (permafrost) soils and other mechanisms. The existence of CO₂ and CH₄ feedback mechanisms are evident in the large CO₂ and CH₄ cycles observed during the ice ages (which were caused by the astronomical cycles of Milankovich) when no human industrial activity existed.

Another concern is how much GW can be induced by an increase of CO₂ or CH₄ atmospheric concentration, this is extremely uncertain. The variability of climate sensitivity to CO₂ demonstrates an even wider sensitivity temperature range [6]. If GHGs are major cause of GW, a climate sensitivity to CO₂ increases with a minimum error of 50% (together with the

²The solubility of a gas in a liquid is directly proportional to the partial pressure of the gas above the liquid: $C = kP_{\text{gas}}$, where C is the solubility of a gas at a fixed temperature in a particular solvent (in units of M or mL gas/L), k is Henry's constant and P_{gas} is the partial pressure of the gas.

extreme aerosol forcing uncertainty); this error is so large because is not well known how to model the major climate feedback mechanisms, e.g., water vapour and clouds.

If the current IPCC climate models do not contain many feedback mechanisms that amplify the effect of a climate RF, the logical conclusion would be that the climate sensitivity to atmospheric CO₂ concentration is currently significantly overestimated by those modes, while the effect of solar input is severely underestimated.

In 1998 and 1999 Mann *et al.* [9, 10] published the first reconstruction of global temperature over the past 1000 years. This paleoclimatic temperature reconstruction is known as the *Hockey Stick*, as shown below.

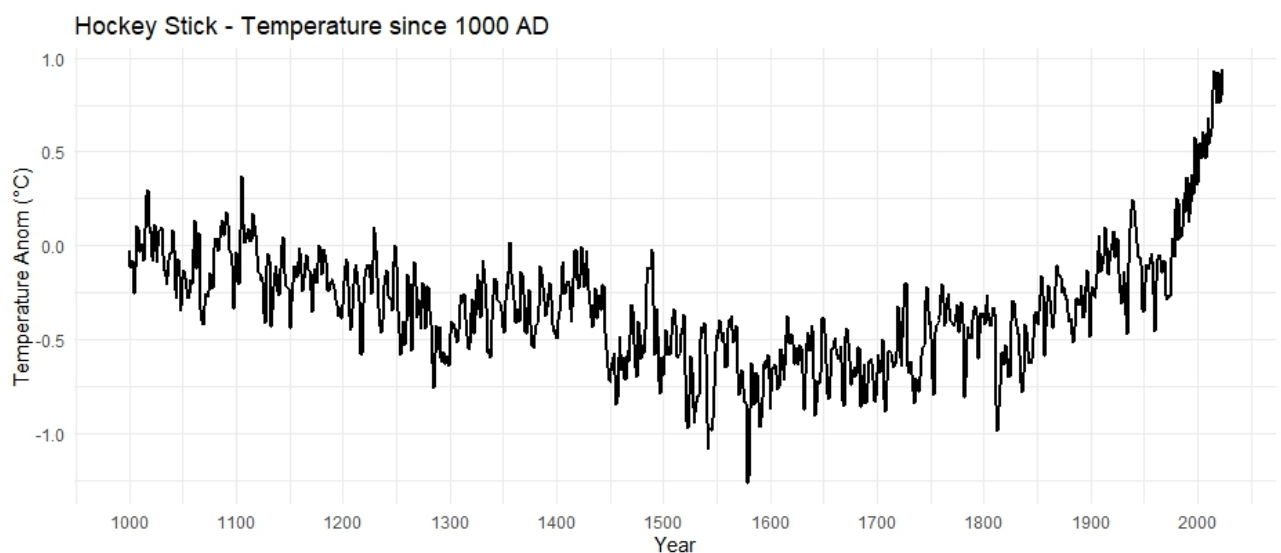


Figure 5.2: Hockey stick shape – since 1000 AD

This paleoclimatic temperature reconstruction shows that before 1900 the average temperature of the planet was almost constant and since 1900 an abnormal warming has occurred. From the medieval Warm Period (1000-1300) and the Little Ice Age (1500-1750) this reconstruction predicts a cooling of less than 0.2 °C. This graph surprised many scientists who have consistently argued that the early centuries of the millennium were quite warm, while the period from 1500 to 1800 was quite cold. It is worth to note that the IPCC's AGWT is based on interpretation of

climate models compatible with the *Hockey Stick* temperature graph. In addition, open issue is whether the tree rings used by Mann are able to accurately reconstruct the temperature changes, especially over long timescales. Tree growth does not depend on temperature alone but on other factors too, such as rain patterns and biological adaptation.

Alternative paleoclimatic reconstructions, which do not use tree rings [13], show a cooling of at least 0.6 °C, three times larger than the *Hockey Stick*.

It is possible to use a phenomenological model to interpret climate change [18]. This model can simulate a typical energy balance model to interpret the GMST. The advantage of the phenomenological approach over that implemented in the traditional climate models, which can be described as analytic engineering, is that the phenomenological approach attempts to measure the climate sensitivity to solar changes through the empirical determination of a kind of *response function*. This methodology would take into account all mechanisms involved in the process, although the individual microscopic mechanisms are not explicitly modelled. The phenomenological approach is essentially a holistic approach that emphasizes the importance of studying a complex macroscopic system by directly analysing the property of the whole because of the complex interdependence of its parts rather than analysing it by separating it into parts.

The limitation with the traditional analytic climate model is that only those mechanisms and physical couplings among them that are well known can be modelled. Therefore, the analytic modularization may fail to properly model and interpret climate change because it just creates a *virtual* climate system that may have nothing to do with reality. In science, the holistic approach complements the traditional analytical approach; essentially, the phenomenological approach acknowledges that understanding climate is an *inverse-problem* that risks to be *ill-posed* in the analytical approach.

The IPCC models assume that the Sun can influence climate only through TSI variations, that is used only as a RF. However, there are additional chemical mechanisms that are stimulated by specific frequencies of the solar radiation (UV alters ozone, which is a GHG, light stimulates photosynthesis which influences the biosphere) and there is an additional modulation of clouds, which alters the

albedo, that is due to solar modulation of cosmic rays flux [22]. The phenomenological model would automatically include all these mechanisms because the climate sensitivity to solar changes is directly, that is phenomenologically, estimated by the magnitude of the temperature patterns that can be recognized as correlated to and, therefore, likely induced by solar changes.

Unfortunately, the uncertainties in the data make it difficult to correctly the climate change. Even the global warming of about 0.8 °C since 1900 may be uncertain. In fact, during this period the land warmed by about 1.1 °C, while the oceans warmed by about 0.6 °C. This difference appears to be too significant to be explained only by different thermal inertia between the ocean and the land regions.

A reasonable alternative is to extract any relevant physical information from the temperature fluctuations. It has been observed that several multi-secular climatic and oceanic records present large cycles with periods of about 50-70 years with an average of 60 years. The existence of a natural 60 year cycle with a total (min-to-max) amplitude of at least 0.3 °C implies that at least 60% of 0.5 °C warming observed since 1970 is due to this cycle. Considering that longer natural cycle can be present and that solar activity was stronger during the second half of the 20th century than during its first half, the natural contribution to the warming since 1970 may have been even larger than 60%. Human emissions can have contributed at most the remaining 40%, or less, of the warming observed since 1970, but the 100% as claimed by IPCC.

If the temperature is characterized by natural periodic cycles the only reasonable explanation is that climate system is modulated by astronomic oscillations. Natural cycles known with certainty are the 11 (Schwabe) and 22 (Hale) year solar cycle, the cycles of the planet and the luni-solar nodal cycles. Jupiter has an orbital period of 11.87 years, Saturn a period of 29.4 years, these periods predict three other major cycles which are associated with both Jupiter and Saturn: about 10 years, the opposition of the planets, about 20 years their synodic cycle³ and about 60 years, the repetition of the combined orbits of the two planets.

³The synodic period is the amount of time that it takes for an object to reappear at the same point in relation to two or more other objects. In common usage, these two objects are typically Earth and the Sun. The time between two successive oppositions or two successive conjunctions is also equal to the synodic period.

These cycles can be used to reconstruct the fluctuations of the temperature, for example, it is possible to adopt a model using only the major 20 and 60 year cycles plus a quadratic trend of the temperature and the reconstruction is obtained. Variations in the Earth's rotation and tides caused by the lunar cycles can drive ocean oscillations, which in turn may alter the climate, in particular the Atlantic Multidecadal Oscillation (AMO) [23] and the Pacific Decadal Oscillation (PDO) present a 60-year cycles and other faster cycles.

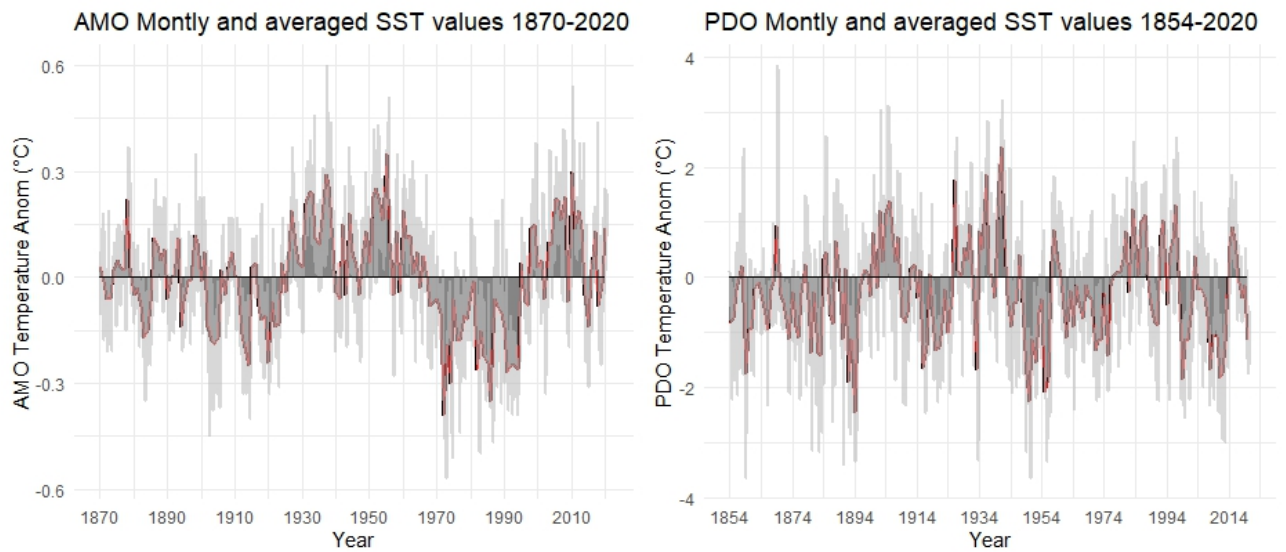


Figure 5.3: AMO and PDO oscillations

The physical mechanisms involved in the process are likely numerous. The gravitational forces of the planets can partially modulate the solar activity; there is also the possibility that the Earth's orbital parameters are directly modulated by the gravitational forces of Jupiter, Saturn and the moon, and the Sun's magnetic force in such a way that the length of day is modulated and/or other planetary parameters are altered. Apparently all these mechanisms have not been kept under consideration in IPCC's models.

CHAPTER 6

RECENT CHANGES IN SOLAR OUTPUTS AND THE GLOBAL MEAN SURFACE¹

6.1 Analysis of contributions to GMAST

For a sudden change in the radiative forcing of the Earth's climate system, the global surface air temperature T would approach its new value exponentially with a time constant

$$\tau = \frac{C_H}{\lambda_S} = \frac{C_H f T}{I_{TS}(1 - A)} = \frac{C_H f}{4\epsilon\sigma T^3}, \quad (6.1)$$

where C_H is the pertinent ('effective') heat capacity that is in immediate thermal contact with the atmosphere; λ_S^{-1} is the equilibrium climate sensitivity; f is the feedback factor ($f > 1$ for positive feedbacks, $f < 1$ for negative feedbacks, with the assumption that f is independent of T); I_{TS} is the TSI; A is the Earth's albedo; ϵ is the Earth's effective planetary long-wave emissivity²; σ is Stefan-Boltzmann constant.

Several multiple regression studies have shown that solar influences on the temperature record can be separated from other factors, ENSO, volcanoes, anthropogenic, by the different spatial patterns that they induce. Hence, the response of the Earth's surface temperature to solar variations is frequency-dependent and the Earth's climate system acts as a low-pass filter to reduce, if not completely remove, the faster variations. In particular, Michaels & Knappenberger [12] detected a solar cycle variation in the residual trend, due to ENSO and volcanoes effects, while other scholars, [2, 3, 8], included TSI as an additional input in their multivariate fits which use temperature

¹Lockwood M., Recent changes in solar outputs and the global mean surface temperature (2008), doi: <https://royalsocietypublishing.org/doi/10.1098/rspa.2007.0348>

²Value for Earth goes from 0.65 to 0.99 and it is defined as the ratio of global mean long-wave flux emitted at the top of the atmosphere to that for a black body with surface temperature T .

anomaly predictors of the form

$$\Delta T_P(t) = k_S \times S(t, \tau_S) + k_V \times V(t, \tau_V) + k_E \times \Delta E(t, \tau_E + L(t)), \quad (6.2)$$

where S is the solar input variation; V is the volcanic aerosol effect³; ΔE is the anomaly of energy exchange between the deep ocean and the surface mixing layer, here quantified by the N3.4 ENSO index; L is a linear drift term to allow for anthropogenic GHG and aerosol emissions (and relative feedbacks); k_S , k_V , k_E are the appropriate weighting (sensitivity) factors.

Note that the equation (6.2) contains the implicit assumption that the responses are independent; hence, for instance, ΔE is independent of V and S , which is not generally valid [1, 17]. In the form of the temperature predictors given in equation (6.1), the input variations are lagged by best-fit lags τ_S , τ_E and τ_V . The temperature anomaly predictors, also given by previous studies, can be slightly modified using convolution⁴, marked with symbol \otimes , while F is a filter response function

$$\begin{aligned} \Delta T_P &= k_S \times [S \otimes F(\tau_S)] + k_V \times [V \otimes F(\tau_V)] + k_E \times [\Delta E \otimes F(\tau_E)] + L = \\ &\Delta T_S + \Delta T_{AOD} + \Delta T_{ENSO} + \Delta T_{LIN}. \end{aligned} \quad (6.3)$$

The low-pass filter is a simple *RC-filter*, providing an exponential response. The variables k_E , k_V , k_S , L , τ_E , τ_V , τ_S are obtained by the best-fit of ΔT_P to the observed GMAST anomaly ΔT_{OBS} to minimize the r.m.s difference between ΔT_P and ΔT_{OBS} .

The following table provides the time constants, sensitivities, correlations and trends for this fit, plus the corresponding results for fits obtained using the PMOD (Physical-meteorological observatory in Davos) and ACRIM (Active Cavity Radiometer Irradiance Monitor) TSI composites for S . The best-fit response time constant for ENSO variation is $\tau_E \approx 0.4$ year and for the volcanic aerosol forcing is $\tau_V \approx 0.6$ year while the solar response time is estimated to $\tau_S \approx 0.8$ year, for both GCR (Galactic Cosmic Rays) input and TSI composites. The best-fit sensitivity factors k_e , k_V and L are almost identical for the three solar inputs.

³Quantified by the global mean atmospheric optical depth, AOD.

⁴For continuous data: $(f \otimes g) = \int_{-\infty}^{+\infty} f(\tau)g(t - \tau) d\tau$.

Table 1. Trends from best fits of temperature predictor T_P (given by equation (1.2)) to the observed value T_{Obs} using the GCR flux, the PMOD TSI composite and the ACRIM TSI composite to quantify the solar input. (The years of the correlation, the correlation coefficient r and the r.m.s. difference between T_P and T_{Obs} are also given.)

solar input	data years	r	$(\Delta T_{\text{Obs}} - \Delta T_P)^2$ (K ²)	trend 1987–2006, $\Delta T/\Delta t$ (10^{-3} K yr ⁻¹) ^a				
				solar $\Delta T_S/\Delta t$	ENSO $\Delta T_{\text{ENSO}}/\Delta t$	volcanic $\Delta T_{\text{AOD}}/\Delta t$	linear L	total $\Delta T_P/\Delta t$
GCR flux	1954–2006	0.887	1.73	-0.26 (-1.3%)	-1.10 (-5.6%)	4.67 (23.9%)	14.70 (75.1%)	18.23 (93.1%)
PMOD TSI	1979–2006	0.878	1.65	-0.71 (-3.6%)	-0.81 (-4.1%)	4.62 (23.6%)	14.78 (75.5%)	18.01 (92.0%)
ACRIM TSI	1979–2006	0.872	1.66	0.61 (3.1%)	-0.99 (-5.1%)	4.64 (23.7%)	14.70 (75.1%)	18.96 (96.9%)

^agiven in brackets as a percentage of the observed trend $\Delta T_{\text{Obs}}/\Delta t = 19.57 \times 10^{-3}$ K yr⁻¹.

Table 2. The best-fit response time constants and sensitivity factors for the fits given in table 1.

solar input	time constant τ (yr)			sensitivity factors				linear term L_D (K yr ⁻¹)
	solar τ_S	ENSO τ_E	volcanic τ_V	solar k_S	ENSO k_E	volcanic k_V (K)		
GCR flux	0.83	0.42	0.58	-10.36×10^{-5} K (counts h ⁻¹) ⁻¹	9.68×10^{-2}	-2.33		14.70×10^{-3}
PMOD TSI	0.80	0.42	0.58	5.07×10^{-2} K (Wm ⁻²) ⁻¹	9.68×10^{-2}	-2.52		14.78×10^{-3}
ACRIM TSI	0.75	0.41	0.58	5.33×10^{-2} K (Wm ⁻²) ⁻¹	9.68×10^{-2}	-2.53		14.70×10^{-3}

Figure 6.1: Table for best-fit responses (M. Lockwood)

In reality, TSI satellite composites since 1978 are not certain either. Two major composites PMOD TSI and ACRIM TSI show a dissonance the former with an almost constant trend from 1980 to 2000 and the latter an increasing trend during these period.

The figure below shows the surface temperature components, rescaled, for visual convenience; curve 'a' is the original surface temperature (curve 'b') minus the volcano (curve 'c') and ENSO (curve 'd') signatures plus the dashed curve for ENSO, while the two dashed curves are the 4 year moving average for curve 'a' and 'd' respectively. The '*' symbols indicate the position of the TSI maxima.

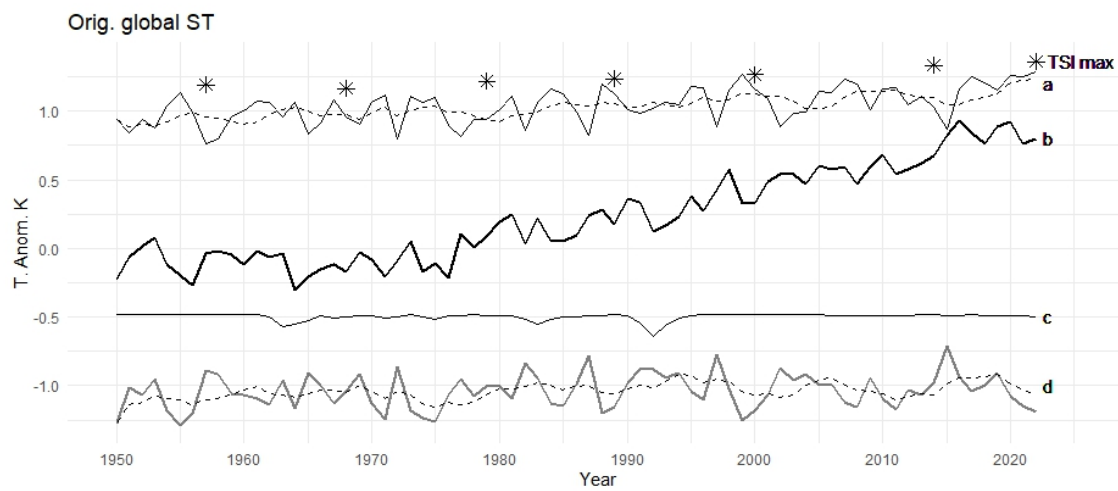


Figure 6.2: Data reconstruction (per year) using Lockwood's parameters

CHAPTER 7

EMPIRICAL ANALYSIS OF THE SOLAR CONTRIBUTION TO GLOBAL MEAN AIR SURFACE TEMPERATURE CHANGE¹

7.1 An empirical climate model with short and long characteristic time responses

It was found that climate is characterized by two major time responses: one short, with a time scale of a few months, $\tau_1 = 0.4 \pm 0.1$ yr, and one long with a time scale that may be as short as $\tau_2 = 8 \pm 2$ yr or, by taking into account statistical biases due to the shortness of the available temperature record, as long as $\tau_2 = 12 \pm 3$ yr. Thus, the climate system appears to be made of two superimposed system characterized with a fast and slow response to the forcings respectively. Consequently, the signature of a given forcing $F(t)$ on the global surface temperature, $\Delta T_F(t)$, is the superposition of at least two meior signals: one generated by the processes with a short time response and the other generated by those processes with a long time response to a forcing. In the case of the solar forcing we should write

$$\Delta T_S(t) = \Delta T_{1S}(t) + \Delta T_{2S}(t), \quad (7.1)$$

where

$$\frac{d\Delta T_{1S}(t)}{dt} = \frac{k_{1S}\Delta I(t) - \Delta T_{1S}(t)}{\tau_{1S}} \implies \Delta T_{1S} = k_{1S}\Delta I(t) - \tau_{1S} \frac{d\Delta T_{1S}(t)}{dt}, \quad (7.2)$$

$$\frac{d\Delta T_{2S}(t)}{dt} = \frac{k_{2S}\Delta I(t) - \Delta T_{2S}(t)}{\tau_{2S}} \implies \Delta T_{2S} = k_{2S}\Delta I(t) - \tau_{2S} \frac{d\Delta T_{2S}(t)}{dt}. \quad (7.3)$$

The parameters τ_{1S} and τ_{2S} are the short and long climate characteristic time responses, whilst k_{1S} and k_{2S} are the average equilibrium climate sensitivities of the two kind of processes.

The above equations assume that the TSI record is used as a *proxy* for the overall sensitivity to

¹Scafetta N., Empirical analysis of the solar contribution to global mean air surface temperature change (2009), doi: <https://doi.org/10.1016/j.jastp.2009.07.007>

solar changes, that is k_{1S} and k_{2S} have the meaning of climate sensitivity to “total solar activity” variation in TSI units.

The climate sensitivity to the 11-year solar cycle is about $Z(11) = 0.11 \pm 0.02 \text{ K/Wm}^{-2}$ [3]; an 11-year solar cycle of about 1 Wm^{-2} causes a peak-to-trough cycle of about 0.1°C on the global surface. Thus, equation (7.1) is solved by the system

$$Z(11) \approx Z_1(11) + Z_2(11), \quad (7.4)$$

$$k_{1S} = Z_1(11) \sqrt{1 + \left(\frac{2\pi\tau_1}{11}\right)^2}, \quad (7.5)$$

$$k_{2S} = Z_2(11) \sqrt{1 + \left(\frac{2\pi\tau_2}{11}\right)^2}, \quad (7.6)$$

where ‘11’ refers to the period of the 11-year solar cycle, $Z_1(11)$ and $Z_2(11)$ are the climate sensitivities to the 11-year solar cycle relative to climate processes with fast and slow characteristic time responses respectively. Considering that for the fast process the parameters have been estimated as shown above, the system can be easily solved and all the parameters can be shown in the table below.

Parameter	Case 1		Case 2	
τ_1	0.4	yr	0.4	yr
τ_2	8	yr	12	yr
k_{1S}	0.053	K/Wm^{-2}	0.053	K/Wm^{-2}
k_{2S}	0.27	K/Wm^{-2}	0.40	K/Wm^{-2}
$k_S = k_{1S} + k_{2S}$	0.32	K/Wm^{-2}	0.45	K/Wm^{-2}
$Z_1(11)$	0.052	K/Wm^{-2}	0.052	K/Wm^{-2}
$Z_2(11)$	0.058	K/Wm^{-2}	0.058	K/Wm^{-2}
$Z(11) = Z_1(11) + Z_2(11)$	0.11	K/Wm^{-2}	0.11	K/Wm^{-2}

Table 7.1: Parameters used in the empirical bi-scale climate model equations for two alternative values of τ_2 .

The conclusion is that even small temperature dependency of the energy balance equation parameters, such as the albedo and emissivity, can amplify the climate sensitivity to solar changes by a large factor [20].

REFERENCES

- [1] J. B. Adams, M. E. Mann, and C. M. Ammann. “Proxy evidence for an El Niño-like response to volcanic forcing”. In: *Nature* 426.6964 (Nov. 2003), pp. 274–278.
- [2] D. H. Douglass and B. D. Clader. “Climate sensitivity of the Earth to solar irradiance”. In: *Geophysical Research Letters* 29.16 (Aug. 2002), pp. 33–1–33–4.
- [3] D. H. Douglass, B. D. Clader, and R. S. Knox. “Climate sensitivity of Earth to solar irradiance: update”. In: *Geophysics* (2004).
- [4] C. Frölich. “Solar irradiance variability since 1978. Revision of the PMOD composite during Solar Cycle 21”. In: *Space Sci Rev* 125(1-4) (2006), pp. 53–65.
- [5] I. Kinnmark. “The Shallow Water Wave Equations: Formulations, Analysis and Application”. In: *Lecture Notes in Engineering* 15 (1985).
- [6] R. Knutti and C. G. Hegerl. “The equilibrium sensitivity to the Earth’s temperature to radiation changes”. In: *Nature Geoscience* 1 (2008), pp. 735–743.
- [7] J. Lean. “Revised ad updated solar irradiance data”. In: *Pers. comm.* (2009).
- [8] J. L. Lean. “Comment on “Estimated solar contribution to the global surface warming using the ACRIM TSI satellite composite” by N. Scafetta and B. J. West”. In: *Geophysical Research Letters* 33.15 (2006).
- [9] M. E. Mann, R. S. Bradley, and M. K. Hughes. “Global-scale temperature patterns and climate forcing over the past six centuries”. In: *Nature* 392 (1998), pp. 779–787.
- [10] M. E. Mann, R. S. Bradley, and M. K. Hughes. “Northern Hemisphere temperatures during the past millennium: inferences, uncertainties and limitations”. In: *Geophysical Research Letters* 26 (1999), pp. 759–762.
- [11] J. C. McWilliams. *Fundamentals of Geophysical Fluid Dynamics*. Cambridge, UK: Cambridge University Press, 2006.
- [12] P. J. Michaels and P. C. Knappenberger. “Natural signals in the MSU lower tropospheric temperature record”. In: *Geophysical Research Letters* 27.18 (Sept. 2000), pp. 2905–2908.

- [13] A. Moberg, D. M. Sonechkin, K. Holmgren, N. M. Datsenko, and W. Karlén. “Highly variable Northern Hemisphere temperature reconstructed from low- and high-resolution proxy data”. In: *Nature* 443 (2005), pp. 613–617.
- [14] C. P. Morice, J. J. Kennedy, N. A. Rayner, J. Winn, E. Hogan, R. Killick, R. Dunn, T. Osborn, P. Jones, and I. Simpson. “An updated assessment of near-surface temperature change from 1850: the HadCRUT5 dataset”. In: *J Geophys Res Atmos* 117 (D8) (2020).
- [15] R. A. Pielke. *Mesoscale Meteorological Modeling*. Academic Press, 2002.
- [16] O. Reynolds. “On the dynamical theory of incompressible fluids and the determination of the criterion”. In: *Phil. Trans. R. Soc. A* (186 1895), pp. 123–164.
- [17] B. D. Santer, T. M. L. Wigley, C. Doutriaux, J. S. Boyle, J. E. Hansen, P. D. Jones, G. A. Meehl, E. Roeckner, S. Sengupta, and K. E. Taylor. “Accounting for the effects of volcanoes and ENSO in comparisons of modeled and observed temperature trends”. In: *Journal of Geophysical Research: Atmospheres* 106.D22 (Nov. 2001), pp. 28033–28059.
- [18] N. Scafetta. “Empirical analysis of the solar contribution to global mean air surface temperature change”. In: *J. of Atm. and So.-Terr. Phys.* 71 (2009), pp. 1916–1923.
- [19] C. D. Schönwiese, A. Walter, and A. W. Brinckmann. “Statistical assessments of anthropogenic and natural global climate forcing. An update”. In: *Meteorologische Zeitschrift* 19 (2010).
- [20] N. J. Shaviv. “Using the oceans as a calorimeter to quantify the solar radiative forcing”. In: *Journal of Geophysical Research: Space Physics* 113.A11 (Nov. 2008), n/a–n/a.
- [21] J. C. et al. Solomon. *Climate Change 2007. The Physical Science Basis*. (Eds.) - Cambridge, UK: Cambridge University Press, 2007, p. 969.
- [22] H. Svensmark, T. Bondo, and J. Svensmark. “Cosmic ray decreases affect atmospheric aerosols and clouds”. In: *Geophys. Res. Lett.* 36.L15101 (2009).
- [23] K. E. Trenberth and D. J. Shea. “Atlantic hurricanes and natural variability in 2005”. In: *Geophysical Research Letters* 33.12 (2006).
- [24] S. Urban and P. Seidelmann. *Explanatory supplement to the astronomical almanac*. 3rd ed. University Science Book, US, Sausalito, United States, 2012.
- [25] M. Wild, D. Folini, M. Hakuba, C. Schär, S. Seneviratne, S. Kato, D. Rutan, C. Ammann, E. Wood, and G. König-Langlo. “The energy balance over land and oceans: An assessment

based on direct observations and CMIP5 climate models”. In: *Clim Dym* 44 (2015), pp. 3393–3429.

APPENDIX A

MAIN CONSTANTS USED IN CLIMATE ANALYSIS

$c = 2.99792 \cdot 10^8$	ms^{-1}	(speed of light in the vacuum)
$h = 6.62607015 \cdot 10^{-34}$	JHz^{-1}	(Planck)
$k = 1.380649 \cdot 10^{-23}$	JK^{-1}	(Boltzmann)
$b = 2.89777196 \cdot 10^{-3}$	mK	(Wien)
$\sigma = 5.67037442 \cdot 10^{-8}$	Wm^2K^{-1}	(Stefan-Boltzmann)
$L = 3.828 \cdot 10^{26}$	W	(Sun luminosity)
$\text{AU} = 1.495978707 \cdot 10^{11}$	m	(1 astronomical unit)
$P = 1.3611 \cdot 10^3$	Wm^{-2}	(solar constant)
$R_{\odot} = 6.969 \cdot 10^8$	m	(solar radius)
$S_{\odot} = 4\pi R_{\odot}^2 = 6.1031 \cdot 10^{18}$	m^2	(area of solar surface)
$T_{\oplus} = 14$	$^{\circ}\text{C}$	(current averaged Earth temperature)
$T_{\oplus\text{K}} = 287$	K	(current averaged Earth temperature in Kelvin)
$\alpha_{\oplus} = 0.294$		(Earth's albedo)
$\mathcal{A} = 0.235$		(atmospheric absorption)
$\mathcal{G} = 59\% = 0.59$		(estimated greenhouse effect)

APPENDIX B

MAIN GREENHOUSE GAS CONSTANTS

$C_0 = 277.15$	ppm	(unperturbed part per million CO ₂ in 1750)
$a_1 = -2.48 \cdot 10^{-7}$	ppm CO ₂	
$b_1 = 7.59 \cdot 10^{-4}$	ppm CO ₂	
$c_1 = -2.1 \cdot 10^{-3}$	ppm CO ₂	
$d_1 = 5.2488$	ppm	
$M_0 = 731.41$	ppb	(unperturbed part per billion MH ₄ in 1750)
$a_2 = -8.96 \cdot 10^{-5}$	ppb MH ₄	
$b_2 = -0.000125$	ppb MH ₄	
$c_2 = 0.0$	ppb MH ₄	
$d_2 = 0.045194$	ppb MH ₄	
$N_0 = 273.87$	ppb	(unperturbed part per billion N ₂ O in 1750)
$a_3 = -0.000342$	ppb N ₂ O	
$b_3 = 0.0002546$	ppb N ₂ O	
$c_3 = -0.000244$	ppb N ₂ O	
$d_3 = 0.12173$	ppb N ₂ O	
$m_{\text{atm}} = 5.148 \cdot 10^{21}$	g	(mass of atmosphere in grams)
$\omega_{\text{mol}} = 44.01$	g	(weight of 1 mole of CO ₂ or N ₂ O in grams)
$\mu_{\text{mol}} = 16.04$	g	(weight of 1 mole of CH ₄ in grams)
$A_{\text{mol}} = 28.97$	g	(molar mass of atmosphere in grams)
$Q_{\text{mol}} = \frac{m_{\text{atm}}}{A_{\text{mol}}} = 1.77701 \cdot 10^{20}$		(quantity of moles in the atmosphere)

$$\mathbf{Q}_{1\text{ppm CO}_2} = \mathbf{Q}_{\text{mol}} \cdot \omega_{\text{mol}} \cdot 10^{-6} = 7.82062 \cdot 10^{15} \quad \text{g} \quad (\text{weight of 1ppm CO}_2 \text{ in grams})$$

$$\mathbf{Q}_{1\text{ppb CH}_4} = \mathbf{Q}_{\text{mol}} \cdot \mu_{\text{mol}} \cdot 10^{-9} = 2.85033 \cdot 10^{12} \quad \text{g} \quad (\text{weight of 1ppb CH}_4 \text{ in grams})$$

$$\mathbf{Q}_{1\text{ppb N}_2\text{O}} = \mathbf{Q}_{\text{mol}} \cdot \omega_{\text{mol}} \cdot 10^{-9} = 7.82062 \cdot 10^{12} \quad \text{g} \quad (\text{weight of 1ppb N}_2\text{O in grams})$$

$$\text{GTons}_X(\text{ppX}) = \frac{\text{ppX}}{\mathbf{Q}_{1\text{ppm}_X} \cdot 10^{-15}} \quad \text{Gt} \quad (\text{ppm/ppb to billion metric tons})$$

APPENDIX C

MAIN FORMULAE USED IN CLIMATE ANALYSIS

$\mathbf{B}_\lambda(\lambda, T) = \frac{2\mathbf{h}\mathbf{c}^2 \lambda^{-5}}{\mathbf{e}^{\frac{\mathbf{h}\mathbf{c}}{\lambda T}} - 1}$	$\text{W sr}^{-1} \text{ m}^{-2} \text{ Hz}^{-1}$	(Planck's law by wavelength per ster.)
$\mathbf{B}_\nu(\nu, T) = \frac{2\mathbf{h} \nu^3 \mathbf{c}^{-2}}{\mathbf{e}^{\frac{\mathbf{h}\nu}{kT}} - 1}$	$\text{W sr}^{-1} \text{ m}^{-2} \text{ Hz}^{-1}$	(Planck's law by frequency per ster.)
$\mathbf{F}(d) = \frac{\mathbf{L}}{4\pi d^2}$	Wm^{-2}	(Flux at distance d from the Sun)
$\mathbf{F}_\lambda(\lambda) = \frac{\mathbf{P} \mathbf{c}}{\lambda^2}$	Wm^{-2}	(Flux by wavelength)
$\mathbf{n}_\lambda(\lambda) = \frac{\mathbf{P} \lambda}{\mathbf{h} \mathbf{c}}$		(number of photons by wavelength)
$\mathbf{s}_b(T) = \sigma T^4$	Wm^{-2}	(Stefan-Boltzmann law - T in Kelvin)
$\mathbf{L}_s(T) = \mathbf{S}_\odot \mathbf{s}_b(T)$	Wm^{-2}	(Sun lum. - T in Kelvin)
$\pi \int_0^{+\infty} \mathbf{B}_\lambda(\lambda, T) d\lambda = 3.83589 \cdot 10^{26} \text{ W}$		(Sun lum. by num. integ. by wavelength)
$\pi \int_0^{+\infty} \mathbf{B}_\nu(\nu, T) d\nu = 3.83589 \cdot 10^{26} \text{ W}$		(Sun lum. via num. integ. by frequency)
$T_\oplus(S) = \sqrt[4]{\frac{1 - \alpha_\oplus - \mathcal{A}}{\sigma(1 - \mathcal{G})}} \cdot S_\odot$	K	(Earth's averaged temperature by TSI)

APPENDIX D

RADIATIVE FORCING INDUCED BY MAIN GREENHOUSE GASES¹

$$\Delta F_{\text{CO}_2}(C, N) = \left[\mathbf{d}_1 + \mathbf{a}_1(C - \mathbf{C}_0) + \mathbf{b}_1(C - \mathbf{C}_0)^2 + \mathbf{c}_1\sqrt{N} \right] \ln \frac{C}{\mathbf{C}_0} \quad \text{Wm}^{-2} \quad (\text{CO}_2 \text{ RF in ppm and N}_2\text{O in ppb})$$

$$\Delta F_{\text{CH}_4}(M, N) = \left(\mathbf{a}_2\sqrt{M} + \mathbf{b}_2\sqrt{N} + \mathbf{d}_2 \right) \left(\sqrt{M} - \sqrt{\mathbf{M}_0} \right) \quad \text{Wm}^{-2} \quad (\text{CH}_4 \text{ RF in ppb and N}_2\text{O in ppb})$$

$$\Delta F_{\text{N}_2\text{O}}(N, M, C) = \left(\mathbf{a}_3\sqrt{C} + \mathbf{b}_3\sqrt{N} + \mathbf{c}_3\sqrt{M} + \mathbf{d}_3 \right) \left(\sqrt{N} - \sqrt{\mathbf{N}_0} \right) \quad \text{Wm}^{-2} \quad (\text{N}_2\text{O RF and CH}_4 \text{ in ppb, CO}_2 \text{ in ppm})$$

¹Global Monitoring Laboratory, *The NOAA annual greenhouse gas index (AGGI)*, 2023, <https://gml.noaa.gov/aggi/aggi.html>.

APPENDIX E

NOTE ABOUT CLIMATE SENSITIVITY PARAMETER

An externally imposed (naturally or human induced) energy imbalance on the Earth's system is termed radiative forcing (ΔF). In a simple global energy imbalance model, the difference between radiative perturbations ΔF and the increased outgoing long-wave radiation that is assumed to be proportional to the surface warming ΔT leads to an increased heat flux ΔQ in the system, such as

$$\Delta Q = \Delta F - \lambda \Delta T.$$

Heat is taken up largely by the oceans, which leads to increasing oceans temperature. The changes in outgoing long-wave radiation that balance the change in forcing are influenced by climate feedbacks. For a constant forcing, the system eventually approaches a new equilibrium where the heat uptake ΔQ is zero and the radiative forcing is balanced by additional emitted long-wave radiation. Commonly the ratio of forcing and equilibrium temperature change $\lambda = \Delta F / \Delta T$ is defined as the climate feedback parameter (in $\text{Wm}^{-2} \text{ } ^\circ\text{C}^{-1}$) and its inverse $k_S = 1/\lambda = \Delta T / \Delta F$ is the climate sensitivity parameter (in $\text{W}^{-1}\text{m}^2 \text{ } ^\circ\text{C}$).